Molecular Therapy
Nucleic Acids
Original Article

Silencing of Carbohydrate Sulfotransferase 15 Hinders Murine Pulmonary Fibrosis Development

Yoshiro Kai,[1] Koichi Tomoda,[1] Hiroyuki Yoneyama,[2] Masahiro Kitabatake,[3] Atsuhiro Nakamura,[1] Toshihiro Ito,[3] Masanori Yoshikawa,[1] and Hiroshi Kimura[1]

[1]Second Department of Internal Medicine, Nara Medical University, Nara 634-8522, Japan; [2]Stelic Institute and Co. Inc., Tokyo 106-0044, Japan; [3]Department of Immunology, Nara Medical University, Nara 634-8522, Japan

Pulmonary fibrosis is a progressive lung disorder characterized by interstitial fibrosis, for which no effective treatments are available. Chondroitin sulfate proteoglycan (CSPG) has been shown to be a mediator, but the specific component of glycosaminoglycan chains of CSPG has not been explored. We show that chondroitin sulfate E-type (CS-E) is involved in fibrogenesis. Small interfering RNA (siRNA) targeting carbohydrate sulfotransferase 15 (CHST15) was designed to inhibit CHST15 mRNA and its product, CS-E. CS-E augments cell contraction and CHST15 siRNA inhibits collagen production. We found that bleomycin treatment increased CHST15 expression in interstitial fibroblasts at day 14. CHST15 siRNA was injected intranasally on days 1, 4, 8, and 11, and CHST15 mRNA was significantly suppressed by day 14. CHST15 siRNA reduced lung CSPG and the grade of fibrosis. CHST15 siRNA repressed the activation of fibroblasts, as evidenced by suppressed expression of α smooth muscle actin (αSMA), connective tissue growth factor (CTGF), lysyl oxidase like 2 (LOXL2), and CC-chemokine ligand 2 (CCL2)/monocyte chemoattractant protein-1 (MCP-1). Inflammatory infiltrates in the bronchoalveolar lavage fluid (BALF) and interstitium were diminished by CHST15 siRNA. These results indicate a pivotal role for CHST15 in fibroblast-mediated lung fibrosis and suggest a possible new therapeutic role for CHST15 siRNA in pulmonary fibrosis.

INTRODUCTION

Pulmonary fibrosis is a diffuse parenchymal lung disorder that occurs in response to a special environmental exposure or occupational pollutants and is related to an underlying connective tissue disease. Idiopathic pulmonary fibrosis (IPF) is a progressive lung disease characterized by progressive dyspnea and worsening pulmonary function, and most patients with IPF die within 5 years of diagnosis.[1] Pathological features of IPF include accumulation of fibroblasts, myofibroblasts, and extracellular matrix (ECM), including proteoglycans (PGs). The etiology of IPF is not fully understood, and no therapeutic strategy has yet been established.

Fibroblasts play a central role in the pathogenesis of IPF by regulating growth factors, such as transforming growth factor-β (TGF-β), connective tissue growth factor (CTGF), and platelet-derived growth factor (PDGF), through excessive deposition of ECM.[2] To reduce the fibrogenesis in IPF, it is important to attenuate activation of fibroblasts and production of these inflammatory cytokines.

PGs are important mediators in inflammation/leukocyte trafficking and regulation of the functions of various growth factors/cytokines.[3] Versican, which is known as a large chondroitin sulfate proteoglycan (CSPG), localized to early fibroblast foci in human lungs affected by IPF.[4] Chondroitin sulfate (CS)/dermatan sulfate was increased in lung biopsies from patients with IPF and in lung tissue from a rat bleomycin model.[5] We reported that deposited CSPGs induced accumulation of macrophages contributing to chronic inflammation and promoting fibrogenesis in a bleomycin-induced fibrosis model. In addition, digestion of CSPGs by the CSPG-digesting enzyme chondroitinase ABC alleviated lung fibrosis and increased survival rates.[6] PGs consist of a core protein to which multiple sulfated glycosaminoglycan (sGAG) side chains are attached. CS chains consist of repeating disaccharides of D-glucuronic acid and N-acetyl-D-galactosamine (GalNAc) and are modified with sulfate groups at C-2 in uronic acid residues, as well as at C-4 and/or C-6 in GalNAc residues. The sulfation pattern of CS is known to be important for the specific functions of CS. We also recently reported that carbohydrate sulfotransferase 3 small interfering RNA (siRNA) diminishes macrophage accumulation, inhibits matrix metalloproteinase-9 expression, and promotes lung recovery in murine pulmonary emphysema.[7]

Carbohydrate sulfotransferase 15 (CHST15), formerly known as N-acetylgalactosamine 4-sulfate 6-O-sulfotransferase (GalNAc4S-6ST), is a special sulfotransferase responsible for biosynthesis of chondroitin sulfate E-type (CS-E) from chondroitin sulfate A-type (CS-A) through transfer of a sulfate group to position C6 of GalNAc ($4SO_4$) in CS-A. CHST15 was purified to homogeneity from squid cartilage containing large amounts of CS-E,[8] and human cDNAs were cloned.[9] CHST15 is responsible for bone marrow-derived mast cell and pulmonary metastasis.[10–12] The effect of CHST15

Received 6 September 2016; accepted 20 December 2016;
http://dx.doi.org/10.1016/j.omtn.2016.12.008.

Correspondence: Yoshiro Kai, Second Department of Internal Medicine, Nara Medical University, 840 Shijo-cho, Nara 634-8522, Japan.
E-mail: y-kai@eco.ocn.ne.jp

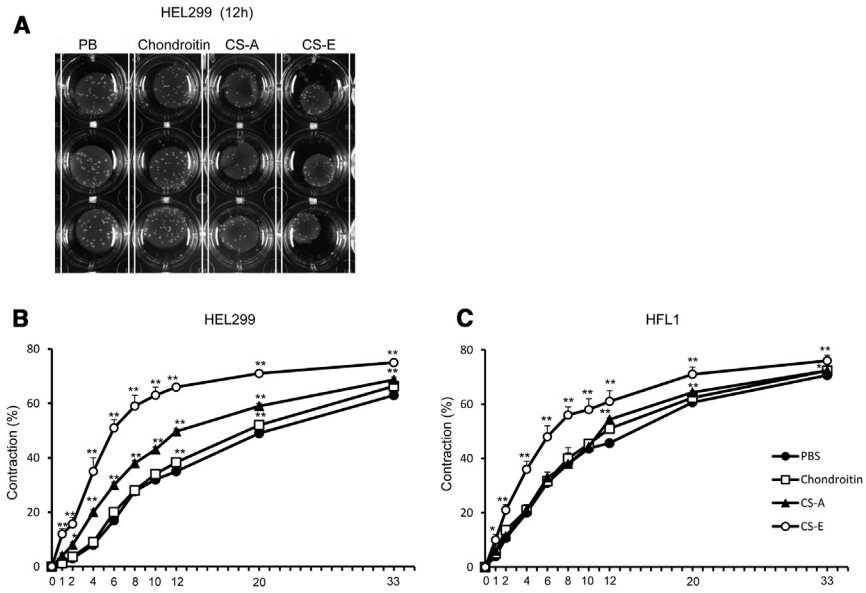

Figure 1. Effect of CS-GAG on Fibroblast-Mediated Collagen Gel Contraction

(A) Representative images of contracting FPCLs after 12 hr in HEL299 cell lines. Gel size was measured with an image analyzer. Contraction of the FPCLs is expressed as the percentage of the gel surface area at t = 0 (time of release). (B) HEL299 cells. (C) HLF1 cells. Results are expressed as the mean ± SD (n = 3). *p < 0.05; **p < 0.01 (versus PBS cultures; Student's t test).

siRNA on fibrosis was reported in rats with dilated cardiomyopathy[13] and in murine colitis models.[14] Furthermore, CHST15 siRNA repressed colonic fibrosis and enhanced mucosal healing in patients with Crohn disease, as shown in the safety and efficacy results of a phase 1 study reported by Suzuki et al.[15] However, the role of CHST15 in the development of lung fibrosis has not yet been explored. Using RNA interference induced by small interfering RNA targeting CHST15, sequence-specific gene silencing was revealed.[16] Prior studies reported that intranasal administration of siRNA is able to downregulate protein expression in the lungs.[17,18]

In summary, this study investigated the potential therapeutic effects of CHST15 siRNA in pulmonary fibrosis, which is a lethal disease.

RESULTS

CS-E Augmented the Collagen Gel Contraction by Human Lung Fibroblasts

Fibroblast-populated collagen lattice (FPCL) assays were performed using different human lung fibroblast cell lines (HEL299 and HFL1) to investigate which type of CS-GAG is involved in fibroblast activation. Gels containing HEL299 and HFL1 fibroblasts were cultured with PBS, chondroitin, CS-A, and CS-E. In HEL299 cell lines, CS-A and CS-E stimulated fibroblast contraction of collagen gels over the observation period. Furthermore, highly sulfated CS-E enhanced fibroblast contraction (Figures 1A and 1B). These results are similar to those observed with HFL1 cell lines (Figure 1C). CS-E stimulates fibroblast contraction of collagen gels.

CHST15 siRNA Inhibited CHST15 mRNA Expression and Collagen Production In Vitro in Lung Fibroblasts

Since CS-E preferentially activated the lung fibroblast cell lines, we focused on CHST15, the sole enzyme that selectively biosynthesizes CS-E, and performed blocking experiments using CHST15 siRNA to investigate whether CHST15 is involved in fibroblast activation. CHST15 siRNA significantly inhibited CHST15 mRNA in HEL299 and HFL1 cells in a dose-dependent manner (Figures 2A and 2B). The effect of CHST15 siRNA was assessed by a collagen synthesis assay in vitro culture system. CHST15 siRNA significantly reduced the amount of collagen production by both lung fibroblast cell lines (Figures 2C and 2D).

CHST15 siRNA Effectively Inhibited CHST15 mRNA Expression In Vivo in Bleomycin-Induced Lung Fibrosis in Mice

We next investigated whether CHST15 is involved in lung fibrosis in vivo in bleomycin-induced lung fibrosis in mice. Mice intratracheally exposed to bleomycin showed a significant increase in CHST15 mRNA in the lung at day 14 compared to sham-treated mice (Figure 3). To assess the effect of CHST15 inhibition on fibrosis, CHST15 siRNA or negative control siRNA was administered intranasally at days 1, 4, 8, and 11 after bleomycin challenge. In contrast, CHST15 siRNA significantly suppressed CHST15 mRNA expression at day 14 compared to control siRNA. These results showed that intranasal CHST15 siRNA effectively inhibited the target gene in the lung without inducing any nonspecific inflammation.

CHST15 siRNA Protected against Bleomycin-Induced Lung Fibrosis

To assess whether CHST15 siRNA possesses anti-fibrotic efficacy, the extent of fibrosis was investigated by both histological and biochemical examinations. In the histological investigation, the alveolar walls were severely thickened and diffuse infiltrations of inflammatory cells were evident at the pulmonary interstitium in response to bleomycin at day 14 by H&E staining (Figure 4A). H&E staining showed that control siRNA did not induce additional inflammation, as the histological findings were similar between only bleomycin-treated mice and control siRNA-treated mice. In addition, collagen deposition and the collapse of the alveolar spaces were also observed at day 14 by Masson trichrome staining (Figure 4B). In contrast, mice treated with CHST15 siRNA showed marked suppression of inflammatory cellular infiltration, as evidenced by reduced thickening of the alveolar

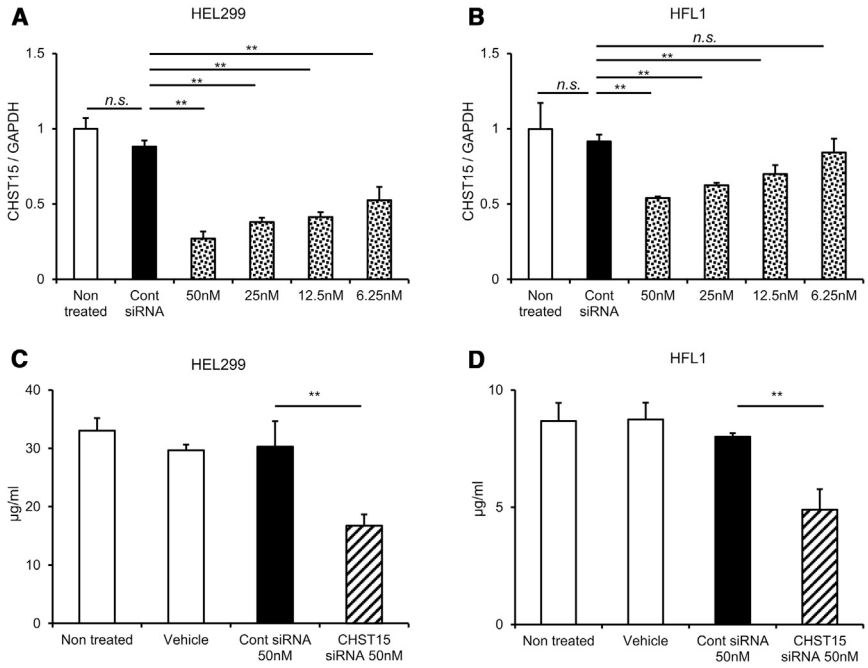

Figure 2. Suppression of CHST15 mRNA Expression and Collagen Production in Human Lung Fibroblasts by CHST15 siRNA

(A and B) Effect of CHST15 siRNA on (A) HEL299 and (B) HFL1 cells. CHST15 mRNA expression in cells after CHST15 siRNA. CHST15 siRNA reduces expression of CHST15 mRNA. (C and D) Quantitative analysis of the effect of CHST15 on collagen production assessed by the Sirius red in vitro culture system on (C) HEL299 and (D) HFL1 cells. Results are expressed as the mean ± SD (n = 3). **p < 0.01 (versus control siRNA; Student's t test). n.s., not significant.

septa and more inflation of the alveoli by H&E staining (Figure 4A). Furthermore, Masson trichrome staining showed that collagen deposition in the alveolar septa was reduced compared to control siRNA mice (Figure 4B). The grade of fibrosis was significantly increased in control siRNA-treated mice, as evidenced by the Ashcroft score, while that of the CHST15 siRNA-treated mice was markedly reduced (Figure 4C). Biochemically, the collagen in the lung was significantly increased after bleomycin treatment. The collagen content in CHST15 siRNA-treated mice was significantly lower than that in control siRNA-treated mice (Figure 4D). Bleomycin induced the loss of air space. However, CHST15 siRNA blocked the loss of air space (Figure 4E).

CHST15 siRNA Inhibited the Expression of CHST15 Protein and sGAG Content in the Lung of Bleomycin-Induced Lung Fibrosis

To examine the distribution and the cell types positive for CHST15, immunohistochemical staining was performed. In sham mice, CHST15 was detected in low levels in the interstitium. In response to bleomycin, the area and extent of CHST15-positive staining was increased in the matrix component, and CHST15 was mainly positive in fibroblasts. CHST15 siRNA effectively suppressed CHST15 expression (Figure 5A).

We then investigated CSPG deposition in the lung using monoclonal antibody (mAb) CS-56, which recognizes an epitope on intact CSPG chains. CSPGs were barely detectable in the sham group but were clearly increased in the fibrotic area 14 days after bleomycin treatment. CHST15 siRNA treatment effectively reduced CSPG deposition (Figure 5B). sGAG deposition was directly evaluated in the lungs using a specific assay. sGAG levels increased 3.8-fold in bleomycin-treated mice by day 14 compared to the sham group. CHST15 siRNA significantly reduced sGAG deposition, thus confirming its in vivo efficacy (Figure 5C). Histological analyses demonstrated that CHST15 siRNA clearly reduced CHST15 protein levels as well as CS-56 in the lung at day 14 compared to the negative control siRNA (Figures 5D and 5E). Thus, CHST15 siRNA suppressed CHST15 mRNA and reduced CHST15 protein and related product CSPG in the injured lung.

CHST15 siRNA Reduced Inflammatory Infiltrate and Accumulation of α Smooth Muscle Actin-Positive Activated Myofibroblasts after Bleomycin Administration

The number of inflammatory cells in the bronchoalveolar lavage fluid (BALF) was further assessed at day 14. Intratracheal bleomycin administration significantly increased the total and differential cell counts in the BALF. CHST15 siRNA-treated mice showed a significant reduction in the number of BALF cells in control siRNA-treated mice (Figure 6A).

We investigated the appearance of F4/80$^+$ macrophages in the lung on day 14. An accumulation of F4/80$^+$ cells was detected on day 14 after bleomycin challenge. However, CHST15 siRNA significantly suppressed the influx of F4/80$^+$ cells (Figures 6B and 6C). Since fibroblasts were hard to detect in the BALF, we stained lung sections with α smooth muscle actin (αSMA), a marker for activated myofibroblasts, to see the effect of CHST15 siRNA on fibroblasts. CHST15 siRNA-treated mice inhibited the increase in the area of αSMA-positive cells in the interstitium compared with control siRNA mice (Figures 6D and 6E).

CHST15 siRNA Inhibited αSMA, CTGF, Lysyl Oxidase-like 2, and CC-Chemokine Ligand 2 mRNA after Bleomycin Administration.

Finally, we examined the expression of fibrosis-related genes in the lung. The expression level of αSMA mRNA was significantly increased in response to bleomycin, and CHST15 siRNA markedly decreased that almost to a normal level, supporting the notion that

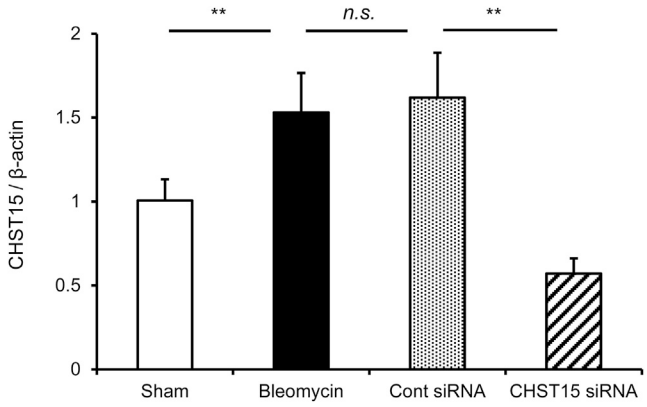

Figure 3. Real-Time qPCR Analysis of CHST15 mRNA in the Lung

Total RNA was isolated from lung tissues on day 14 after bleomycin administration (n = 3–4). Statistical analyses are shown as follows: sham versus bleomycin-only disease control, bleomycin-only versus negative control siRNA, and negative control siRNA versus CHST15 siRNA. Results are expressed as the mean ± SD. **$p < 0.01$ (Student's t test). n.s., not significant.

CHST15 siRNA reduced the activation status of fibroblasts in the inflamed lung at day 14 (Figure 7A). CTGF and lysyl oxidase-like 2 (LOXL2) are mainly produced by the activated fibroblasts and are involved in the pathogenesis of fibrosis.[19–22] CHST15 siRNA also significantly reduced CTGF and LOXL2 mRNA in lung tissues compared to control siRNA (Figures 7B and 7C). CC-chemokine ligand 2 (CCL2)/monocyte chemoattractant protein-1 (MCP-1) is produced by macrophages and fibroblasts and is involved in the recruitment and activation of both macrophages and fibroblasts.[23,24] CHST15 siRNA significantly reduced CCL2 mRNA in lung tissues compared to control siRNA (Figure 7D).

Survival Analysis

Kaplan-Meier survival curves demonstrated that bleomycin mice treated with CHST15 siRNA had a significantly higher survival rate than those given control siRNA (Figure 8).

DISCUSSION

We previously demonstrated that digestion of CSPG by chondroitinase ABC attenuated pulmonary fibrosis in mice.[6] Given the potential of CSPG as a new therapeutic target, we initially investigated which type of CS is critically involved in pulmonary fibrosis. Since CSPG is mainly produced by fibroblasts,[25] we set out to determine the effects of sulfated CS on activation of two independent lung fibroblast cell lines in vitro. Highly sulfated CS-E significantly enhanced fibroblast contraction in FPCL assays, indicating the importance of sulfation, especially CS-E, in activation of lung fibroblasts (Figure 1). CS-E was shown to act as a co-receptor for Wnt and a direct receptor for the receptor for advanced glycation end-products (RAGE).[26] Since the activation of human lung fibroblasts including HLF cells is mediated by RAGE[27] and Wnt,[28] it is thought that CS-E activates fibroblasts at least through RAGE and/or Frizzled pathways. Interestingly, lung fibroblasts themselves express CHST15, a specific producer of CS-E. Blockade of CHST15 reduced collagen synthesis by fibroblasts, suggesting that CHST15 provides signals to synthesize collagen as well as CS-E in lung fibroblasts (Figure 2). Therefore, CHST15/CS-E can be thought to activate fibrosis pathways in an autocrine and/or paracrine manner.

From a clinical perspective, selective inhibition of CS-E by a specific enzyme, antibody (Ab), or oligosaccharide is still difficult. We therefore conducted functional blocking experiments using CHST15 siRNA to selectively inhibit the synthesis of CS-E. In mouse lung fibrosis models, $CHST15^+$ cells were barely detected in normal lungs but increased within the interstitium and fibrotic lesions. In morphology, fibroblasts were the main producers of CHST15 protein at the fibrosis phase (Figure 5A). Significant deposition of CS chains was detected within the interstitium and fibrotic lesions as well (Figure 5B). Here, fibroblasts were also judged to be the main producer. Intranasal administration of siRNA effectively inhibited expression of both CHST15 mRNA and protein in vivo (Figures 3 and 5A and 5D). CHST15 siRNA reduced CSPG in the interstitium and fibrotic lesions (Figures 5B and 5E). Administration of synthetic siRNA has the potential to active the innate immune response and lead to increased secretion of inflammatory cytokines and interferons.[29] There were no significant differences in inflammatory parameters such as BALF total cell count, differential cell count, and inflammatory cytokine mRNA levels between control siRNA-treated and untreated bleomycin-administered mice, suggesting that intranasal instillation of siRNA did not induce nonspecific inflammation in vivo (Figures 6A–6C and 7). The direct administration of naked siRNA into the airway would therefore seem to be an effective and safe application.

CHST15 siRNA significantly reduced the grade of fibrosis, blocked the loss of air space, and improved survival (Figures 4 and 8). Increased interstitial space consists of a diffuse $CS\text{-}56^+$ area (average 34.4%), focal αSMA^+ cells, (average 21.5%), and $CHST15^+$ cells (average 7.3%) in quantitative histological analyses. This suggests that part of αSMA^+-activated fibroblasts express CHST15 and produce CS into the matrix space. CHST15 siRNA reduced the area of αSMA^+-activated fibroblasts (Figures 6D and 6E), indicating inhibited accumulation of activated fibroblasts. It is still unclear whether the mechanism is based on inhibited recruitment of fibrocytes from the circulation, inhibited epithelial-mesenchymal transition (EMT), or inhibited activation of resident fibroblasts. However, mRNAs for αSMA and CTGF were significantly reduced by CHST15 siRNA, indicating that CHST15 siRNA participates in at least activation of lung fibroblasts of any origin, leading to an increased number of αSMA^+-activated fibroblasts. CHST15 siRNA possesses fibrinolytic activity, as evidenced by the significant suppression of LOXL2 (Figure 7C). Thus, CHST15 siRNA represses fibrogenic activity and enhances fibrinolytic activity of fibroblasts, leading to reduced fibrosis while strengthening the air space.

CHST15 siRNA also showed anti-inflammatory action, as the accumulation of macrophages in the BALF and interstitium was

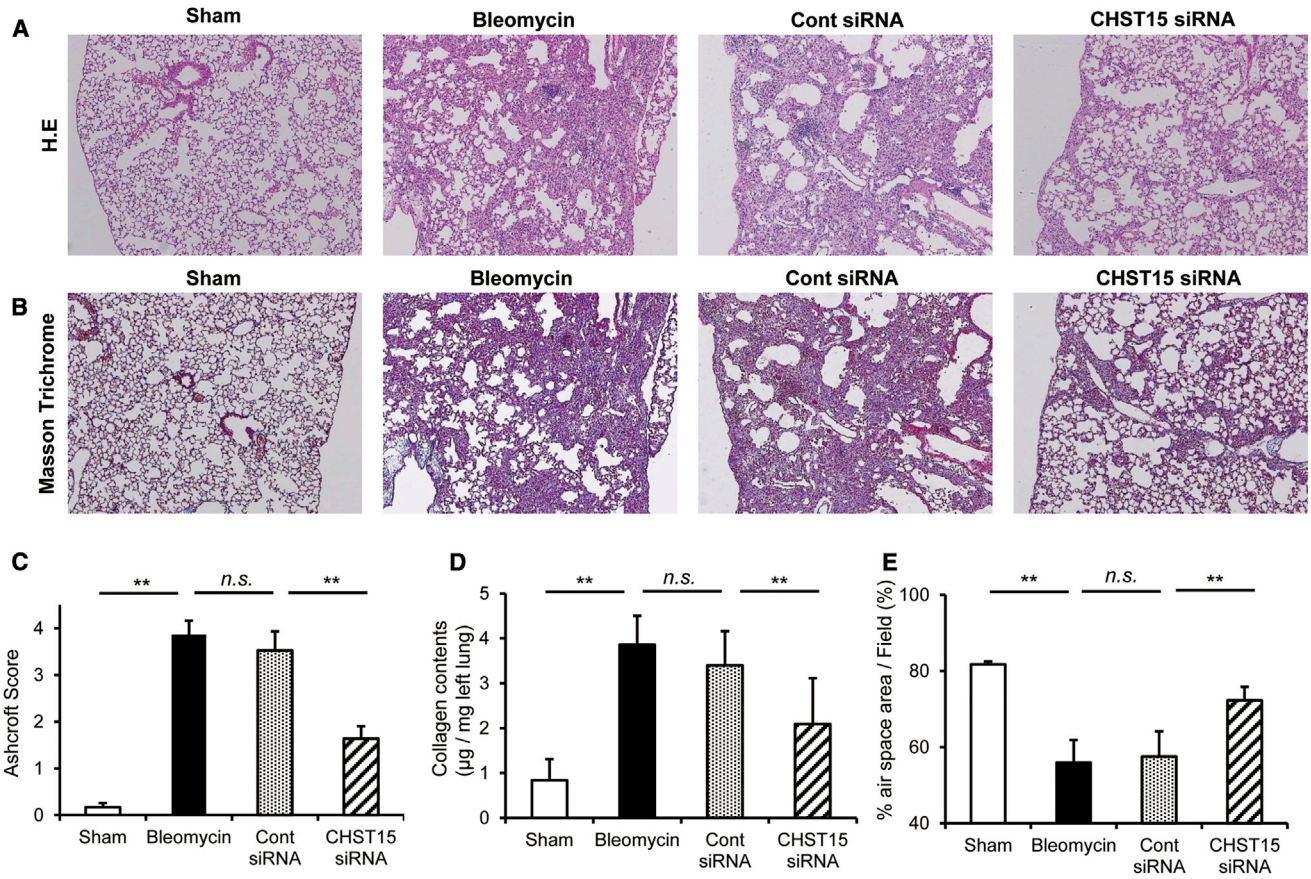

Figure 4. Protective Effect of CHST15 siRNA in Bleomycin-Induced Pulmonary Fibrosis

(A) H&E staining of lung tissue 14 days after bleomycin administration. Bleomycin-induced pulmonary fibrosis was attenuated by treatment with CHST15 siRNA. (B) Masson trichrome staining of lung tissue 14 days after bleomycin administration. (C) Semiquantitative analysis of lung fibrosis on day 14 using the Ashcroft score (n = 5–9). (D) Collagen content of left lungs on day 14 after bleomycin administration. CHST15 siRNA significantly decreased the amount of collagen (n = 5–10). (E) Percentage of air space area in lung sections on day 14 after bleomycin administration (n = 5). Statistical analyses are shown as follows: sham versus bleomycin-only disease control, bleomycin-only versus negative control siRNA, and negative control siRNA versus CHST15 siRNA. Results are expressed as the mean ± SD. **$p < 0.01$ (Student's t test). Magnification, × 100 in (A) and (B). n.s., not significant.

significantly decreased. We previously reported that the accumulation of macrophages in the BALF and interstitium contributes to engaged inflammation and fibrosis through CSPG-CD44 interaction.[6] CSPGs provide a scaffold for $CD44^+$ macrophages, leading to persistent inflammation. In this study, CHST15 effectively reduced CSPG deposition in the interstitium. This suggests that the anti-inflammatory action of CHST15 siRNA was attributable in part to decreased scaffolding of macrophages. In addition, CHST15 siRNA reduced CCL2 mRNA in lung tissues CCL2 is expressed by both fibroblasts and macrophages,[6,30,31] decreased CCL2 expression may be due to decreased accumulation of both cell types.

The treatment of IPF has changed from anti-inflammatory drugs (e.g., corticosteroids) and immunosuppressants to anti-fibrotic drugs. Recently, pirfenidone and nintedanib have entered the mainstream of IPF treatment.[32] Although fibrosis is called the end stage of chronic inflammation in specific organs (e.g., liver cirrhosis), fibrosis is one phenotype of the living body's ongoing protective reaction. Our proposed mechanism of CHST15/CS-E in the pathogenesis of lung fibrosis is as follows: epithelial damage induced by bleomycin may provide signals to trigger fibroblast activation. Activated fibroblasts enhance CHST15 expression and produce both CS-E and collagen in the interstitium. CSPG containing CS-E may provide a scaffold to activated fibroblasts as well as macrophages at least through CD44. CS-E further activates fibroblasts themselves partly through RAGE and/or Wnt signaling, leading to persistent activation of fibrogenesis pathways. CHST15 siRNA blocked the fibrogenic cycle induced by CHST15/CS-E and inhibited LOXL2-mediated cross-linking of collagen-fibers, leading to decreased fibrosis.

The following limitations were identified in this study. First, we did not evaluate the effect of CHST15 siRNA after fibrosis was established. In this respect, CHST15 siRNA has the potential to promote a LOXL2-related fibrinolytic effect. Together with previous results

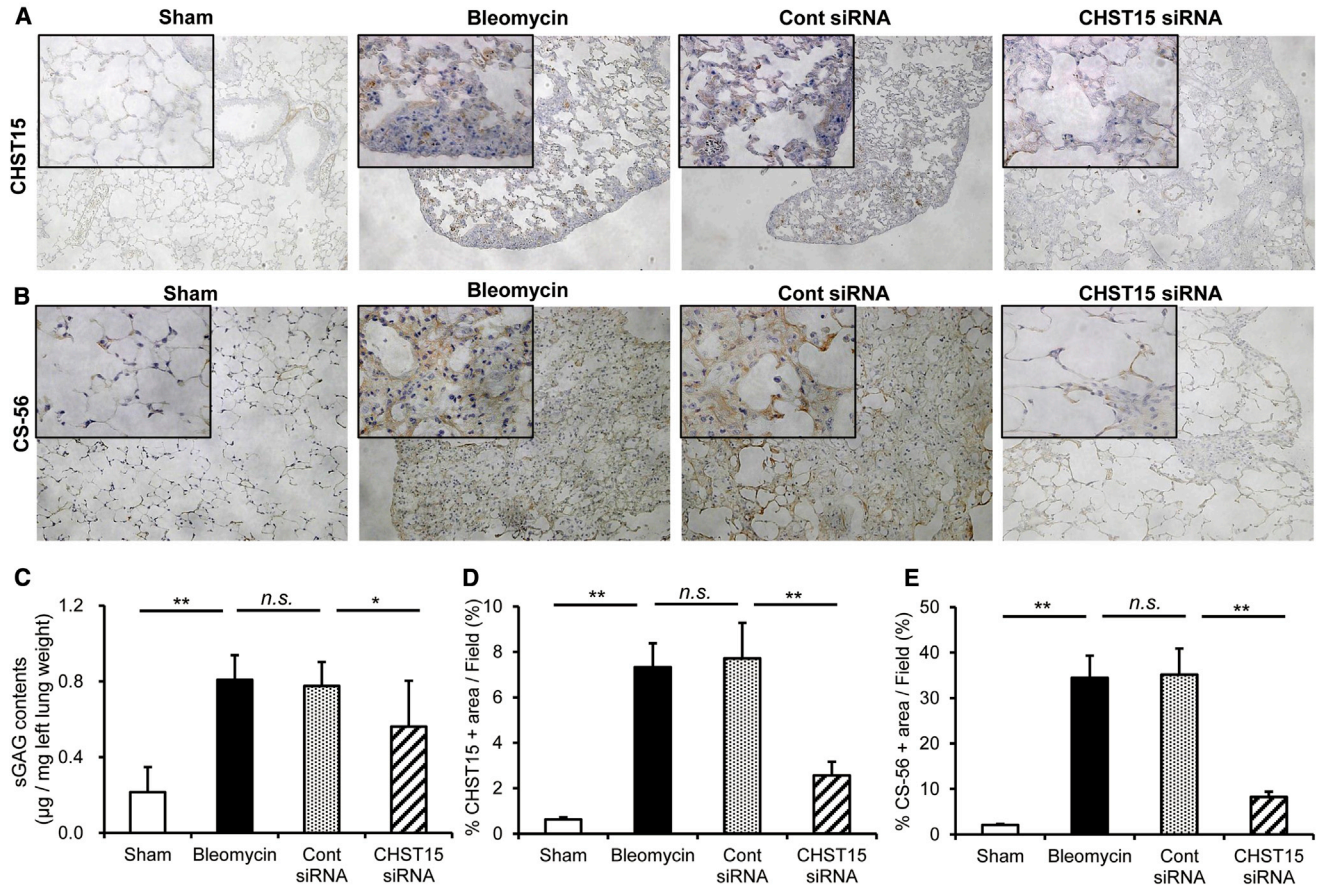

Figure 5. CHST15 siRNA Inhibited the Expression of CHST15 Protein and CS56 In Vivo

(A) Immunohistochemical detection of CHST15 on day 14. (B) Immunohistochemical detection of CSPGs on day 14. CS-56 recognizes an epitope on intact chondroitin sulfate glycosaminoglycan chains. CS-56 immunolabeling indicated that CHST15 siRNA treatment suppressed the increased chondroitin sulfate after bleomycin administration. (C) sGAG content of the left lung on day 14 after bleomycin administration (n = 5–12). (D) Percentage of CHST15-positive area in lung sections on day 14 after bleomycin administration (n = 5). (E) Percentage of CS-56-positive area in lung sections on day 14 after bleomycin administration (n = 5). Statistical analyses are shown as follows: sham versus bleomycin-only disease control, bleomycin-only versus negative control siRNA, and negative control siRNA versus CHST15 siRNA. Results are expressed as the mean ± SD. *$p < 0.05$; **$p < 0.01$ (Student's t test). Magnification, ×100 in main image and ×400 in top-left image in (A) and (B). n.s., not significant.

that show that highly sulfated CSPG acts as an obstacle to lung recovery.[7] Delayed therapy is scheduled for future research. Second, using immunohistology, we evaluated CSPG deposits by CS-56 antibodies but not by a specific CS-E antibody, because of the lack of availability of a highly specific antibody to detect only CS-E. However, we performed immunostaining for CHST15, which is the sole protein that can synthesize CS-E, and we directly showed a reduction of the CHST15 protein. In addition, chemical assays also showed reduced sulfation of GAG. Thus, reduced CHST15 protein may contribute to reduced sulfation of GAG in the lungs, strongly suggesting the reduction of CS-E among sGAG.

In summary, siRNA targeting CHST15 attenuated the development of bleomycin-induced pulmonary fibrosis in mice. Furthermore, siRNA targeting CHST15 inhibited fibrosis-related genes, including αSMA, CTGF, LOXL2, and CCL2. CHST15 appears to be a potential therapeutic target for the treatment of pulmonary fibrosis.

MATERIALS AND METHODS

Cell Culture

HEL299 and HFL1 human lung fibroblast cell lines were purchased from American Type Culture Collection (ATCC). Cells were grown in DMEM (Sigma-Aldrich) supplemented with 10% fetal calf serum and 1% antibiotics (penicillin and streptomycin) and were incubated at 37°C in a humidified chamber with 5% CO_2.

FPCL Contraction Assay

Collagen lattices were polymerized in 24-well tissue culture trays. HEL299 or HFL1 cells were mixed with 2.7 mg/mL Cellmatrix type I-A (Nitta Gelatin) to yield a final volume of 500 μL containing

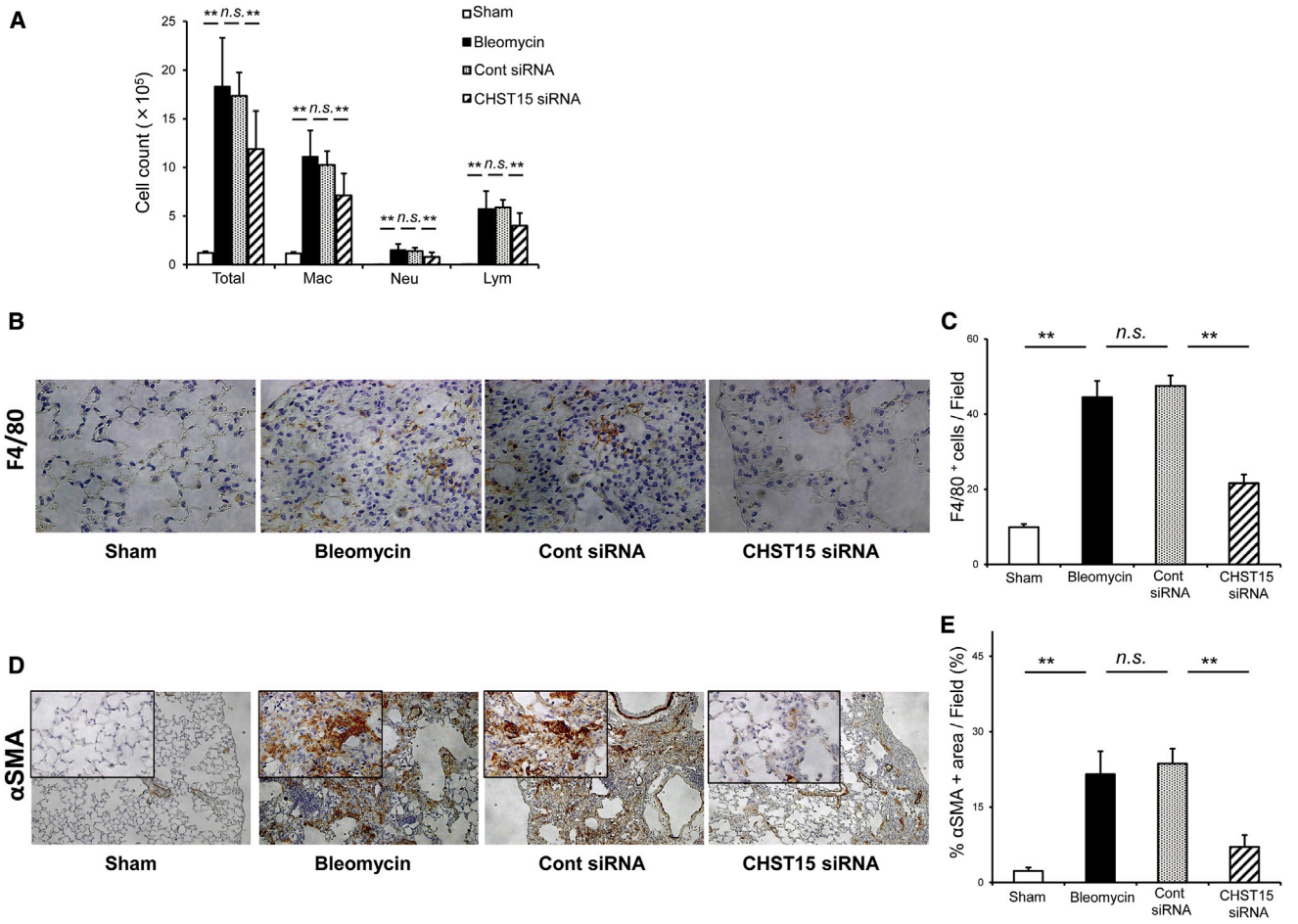

Figure 6. Repression of Inflammatory Infiltrate and Accumulation of αSMA-Positive Activated Myofibroblasts by CHST15 siRNA after Bleomycin Administration

(A) Effect of CHST15 siRNA on the infiltration of total and differential cell counts in bronchoalveolar lavage fluid on day 14 (n = 5–14). (B) Lung sections after bleomycin administration on day 14 were stained with F4/80. (C) Quantitative analysis of F4/80$^+$ cells on day 14 after bleomycin administration. (D) Lung sections after bleomycin administration on day 14 were stained with αSMA. (E) Percentage of αSMA-positive area in lung sections on day 14 after bleomycin administration (n = 5). Statistical analyses are shown as follows: sham versus bleomycin-only disease control, bleomycin-only versus negative control siRNA, and negative control siRNA versus CHST15 siRNA. Results are expressed as the mean ± SD. **$p < 0.01$ (Student's t test). Magnification, ×200 in (B); ×100 in main image and ×400 in top-left image in (D). n.s., not significant.

4×10^5 cells with PBS and 0.1 mg/mL chondroitin, CS-A, or CS-E (Seikagaku). The gels were cultured for 60 minutes, at which time they were mechanically released. Digital images of the floating lattices were captured at timed intervals up to 33 hr after release. Collagen lattice areas were quantified using ImageJ software (NIH), and sequential area calculations were normalized to the area measured immediately after release. Each assay was done in triplicate.

Transfection of siRNA

RNA interference was performed using the reverse transfection method and siRNA for CHST15, and negative control siRNA was designed to target the coding sequence of human CHST15 as described previously.[33] HEL299 cells and HFL1 cells, CHST15 siRNA (6.25, 12.5, 25, or 50 nM) or negative control siRNA, Lipofectamine 2000, and Opti-MEM medium (Invitrogen) were mixed and incubated according to the manufacturer's instructions. After 48-hr transfection, the cells and culture supernatant were collected.

qRT-PCR, In Vitro Study Collagen Contents

Total RNA was extracted from culture cells by homogenization using RNAiso Plus (Takara Bio) and the SV Total RNA Isolation kit (Promega) and was reverse transcribed as previously described.[33] Real-time PCR was performed using real-time PCR DICE and SYBR Premix Taq (Takara Bio). To calculate the relative mRNA expression level, the expression of each gene was normalized to that of the reference gene. The primers for real-time RT-PCR were designed as previously reported.[33] The supernatant of the cell culture was measured using a Sircol Collagen Assay kit (Biocolor) according to the manufacturer's instructions.

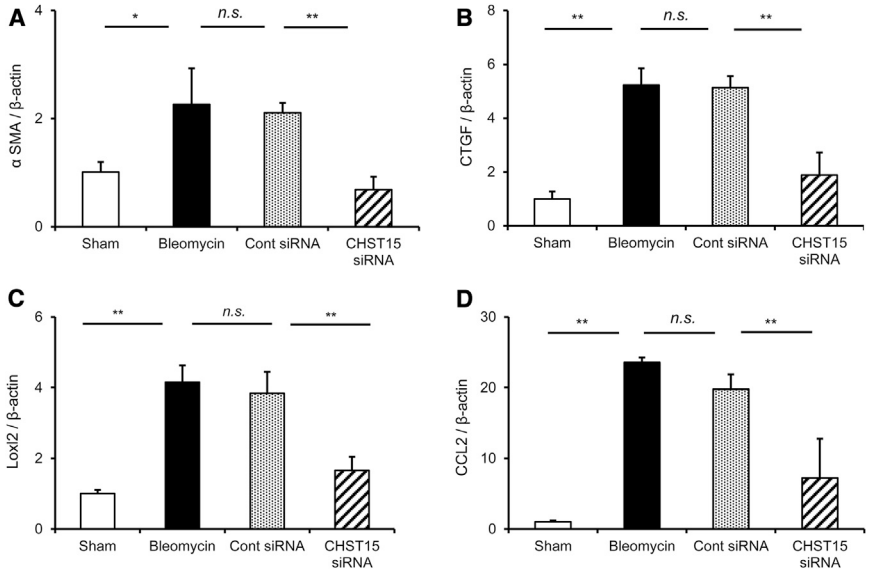

Figure 7. Suppression of Fibrosis-Related Gene Expression in the Lung by CHST15 siRNA

(A–D) Real-time qPCR analysis of (A) αSMA, (B) CTGF, (C) LOXL2, and (D) CCL2. Total RNA was isolated from lung tissues on day 14 (n = 3–4). Statistical analyses are shown as follows: sham versus bleomycin-only disease control, bleomycin-only versus negative control siRNA, and negative control siRNA versus CHST15 siRNA. Results are expressed as the mean ± SD. *$p < 0.05$; **$p < 0.01$ (Student's t test). n.s., not significant.

Mice

Pathogen-free female C57BL/6 (6- to 8-week-old) mice were obtained from SLC Japan and bred in a pathogen-free facility in the laboratory animal research center at Nara Medical University. All experiments were carried out under the control of our committee and complied with the Guidelines for Animal Experiments of Nara Medical University and with the Guideline Principles for the Care and Use of Laboratory Animals approved by the Japanese Pharmacological Society.

Animal Model

Mice were anesthetized by isoflurane inhalation and were administered either 2 mg/kg bleomycin sulfate (LKT Laboratories), or saline only, intratracheally in a volume of 50 μL. A 2-μM injection (injection volume, 50 μL) of CHST15 siRNA (Silencer Pre-designed siRNA, catalog no. 4390815; Ambion) or negative control siRNA (Silencer Negative Control siRNA 1, catalog no. AM4611; Ambion) was dissolved in RNase-free water and administered intranasally after anesthetization by isoflurane inhalation on days 1, 4, 8, and 11. This protocol resulted in the creation of four groups: sham mice given negative control siRNA (sham group), bleomycin mice given vehicle (bleomycin group), bleomycin mice given negative control siRNA (cont siRNA group), and bleomycin mice treated with CHST15 siRNA (CHST15 siRNA group).

Histological Examination

The lungs were fixed in neutral-buffered 10% formalin (Wako Pure Chemical Industries). The tissue was embedded in paraffin, and 4-μm-thick sections were stained with H&E and Masson trichrome stain. The Ashcroft score was used for semiquantification of fibrosis severity.[34] Twenty fields were analyzed to review each section. The severity of fibrotic changes in microscopic lung sections was assessed as the mean score for the observed fields in each section. To quantify the air space area, bright-field images of H&E staining were captured using a digital camera (DFC280; Leica Microsystems) at 100-fold magnification and the negative areas in five fields per section were measured using ImageJ software.

Analysis of Bronchoalveolar Lavage Fluid

Mice were anesthetized by intraperitoneal injection with sodium pentobarbital (50 mg/kg) and the BALF was obtained by flushing the lung via the trachea three times with 0.8 mL sterile PBS. After we counted the number of cells in the BALF with a hemocytometer, we determined cell differentials in cytospin preparations stained with Diff-Quik products (Baxter).

Antibodies and Immunohistochemistry

The following primary Abs were used: CHST15 (GeneTex), F4/80 (Serotec), and αSMA (Dakop) for paraffin-embedded sections and CS-56 (Seikagaku) for frozen sections. Frozen lung sections were prepared as described previously.[35] CS-56 recognizes an epitope on some intact chondroitin sulfate glycosaminoglycan chains. Immunolabeling for F4/80 was performed as reported earlier.[7,36] Immunolabeling for CHST15 was performed with anti-human CHST15 Ab followed by EnVision+ System horseradish peroxidase (HRP)-labeled anti-rabbit polymer (Dako) after antigen retrieval, incubation of the lung section with Target Retrieval Solution (pH 9; Dako) for 15 minutes at 121°C, and staining with 3,3′-diaminobenzidine (Dako). Immunolabeling for CS-56 and αSMA was performed using a Histofine kit (Nichirei Bioscience) according to the manufacturer's instructions. The number of $F4/80^+$ cells was determined using light microscopy in at least 20 randomly chosen high-power fields.[6,36] For quantification of immunostained areas (CHST15, CS-56, and αSMA), bright-field images were captured using a digital camera at 100-fold magnification and the positive areas in five fields per section were measured using ImageJ software.[14,37]

Measurement of Lung Collagen and sGAG Content

The total collagen content of the left lung was measured in each group at 14 days after bleomycin administration using a Sircol Collagen Assay kit (Biocolor) according to the manufacturer's instructions, as described previously.[38] The sGAG content of the left lung was measured using an Alcian blue binding assay for detection of sulfated glycosaminoglycans (Euro Diagnostica) according to the manufacturer's instructions. Collagen content and sGAG content were adjusted by lung weight.

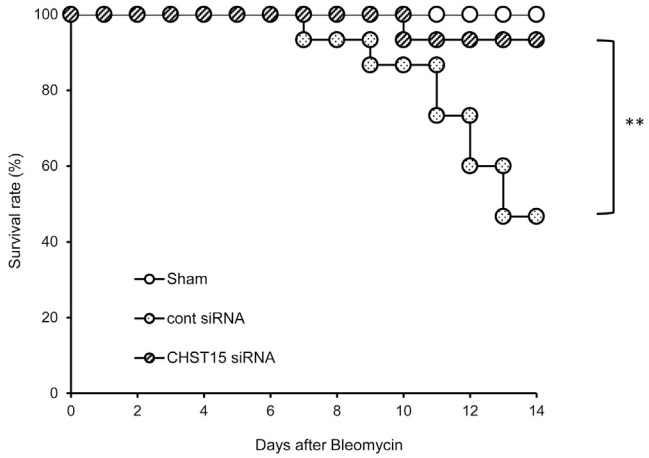

Figure 8. Kaplan-Meier Survival Curves

Bleomycin mice treated with CHST15 siRNA had a significantly higher survival rate than those given control siRNA. **p < 0.01 (long-rank test).

qRT-PCR In Vivo

Total RNA was extracted from lung homogenates using NucleoSpin RNA (Macherey-Nagel) and was reverse transcribed using SuperScript IV Reverse Transcriptase (Invitrogen). αSMA, CTGF, LOXL2, and CCL2 mRNAs were quantified by real-time RT-PCR using a TaqMan gene expression assay in a 7300 Fast Real-Time PCR System (Applied Biosystems). To calculate the relative mRNA expression level, the expression of each gene was normalized to that of the reference gene (β-actin).

Survival Analysis

To evaluate the effect of CHST15 siRNA on survival in bleomycin-injected mice, the sham, control siRNA, and CHST15 siRNA groups were monitored for survival. Survival was estimated from the date of bleomycin administration to the death of mice or 14 days after administration.

Statistical Analysis

Statistical analysis of between-group differences was evaluated using the Student's t test. Survival curves were derived by the Kaplan-Meier method and compared by the log-rank test. A p value less than 0.05 was considered to indicate a statistically significant difference.

AUTHOR CONTRIBUTIONS

Y.K. contributed to the conception and design of the study; contributed to the acquisition, analysis, and interpretation of the data; and drafted the submitted manuscript. K.T. contributed to the analysis and interpretation of the data and to revision of the manuscript. H.Y. contributed to the conception, analysis, and interpretation of the data and revision of the manuscript. M.K. contributed to the laboratory work, acquisition of the data, and revision of the manuscript. A.N. contributed to the laboratory work, acquisition of the data, and revision of the manuscript. T.I. contributed to interpretation of the data and revision of the manuscript. M.Y. contributed to interpretation of the data and revision of the manuscript. H.K. contributed to the supervision of the study and revision of the manuscript.

CONFLICTS OF INTEREST

The authors declare no conflicts of interest.

ACKNOWLEDGMENTS

The authors thank J. Patrick Barron, Professor Emeritus of Tokyo Medical University, for his pro bono review of this manuscript. They also thank Francesco Bolstad, Professor of Clinical English at Nara Medical University, for reviewing the manuscript.

REFERENCES

1. Cordier, J.F., and Cottin, V. (2013). Neglected evidence in idiopathic pulmonary fibrosis: from history to earlier diagnosis. Eur. Respir. J. *42*, 916–923.
2. Bagnato, G., and Harari, S. (2015). Cellular interactions in the pathogenesis of interstitial lung diseases. Eur. Respir. Rev. *24*, 102–114.
3. Mizumoto, S., Fongmoon, D., and Sugahara, K. (2013). Interaction of chondroitin sulfate and dermatan sulfate from various biological sources with heparin-binding growth factors and cytokines. Glycoconj. J. *30*, 619–632.
4. Bensadoun, E.S., Burke, A.K., Hogg, J.C., and Roberts, C.R. (1996). Proteoglycan deposition in pulmonary fibrosis. Am. J. Respir. Crit. Care Med. *154*, 1819–1828.
5. Venkatesan, N., Ouzzine, M., Kolb, M., Netter, P., and Ludwig, M.S. (2011). Increased deposition of chondroitin/dermatan sulfate glycosaminoglycan and upregulation of β1,3-glucuronosyltransferase I in pulmonary fibrosis. Am. J. Physiol. Lung Cell. Mol. Physiol. *300*, L191–L203.
6. Kai, Y., Yoneyama, H., Koyama, J., Hamada, K., Kimura, H., and Matsushima, K. (2007). Treatment with chondroitinase ABC alleviates bleomycin-induced pulmonary fibrosis. Med. Mol. Morphol. *40*, 128–140.
7. Kai, Y., Tomoda, K., Yoneyama, H., Yoshikawa, M., and Kimura, H. (2015). RNA interference targeting carbohydrate sulfotransferase 3 diminishes macrophage accumulation, inhibits MMP-9 expression and promotes lung recovery in murine pulmonary emphysema. Respir. Res. *16*, 146.
8. Ito, Y., and Habuchi, O. (2000). Purification and characterization of N-acetylgalactosamine 4-sulfate 6-O-sulfotransferase from the squid cartilage. J. Biol. Chem. *275*, 34728–34736.
9. Ohtake, S., Ito, Y., Fukuta, M., and Habuchi, O. (2001). Human N-acetylgalactosamine 4-sulfate 6-O-sulfotransferase cDNA is related to human B cell recombination activating gene-associated gene. J. Biol. Chem. *276*, 43894–43900.
10. Ohtake-Niimi, S., Kondo, S., Ito, T., Kakehi, S., Ohta, T., Habuchi, H., Kimata, K., and Habuchi, O. (2010). Mice deficient in N-acetylgalactosamine 4-sulfate 6-O-sulfotransferase are unable to synthesize chondroitin/dermatan sulfate containing N-acetylgalactosamine 4,6-bissulfate residues and exhibit decreased protease activity in bone marrow-derived mast cells. J. Biol. Chem. *285*, 20793–20805.
11. Mizumoto, S., Watanabe, M., Yamada, S., and Sugahara, K. (2013). Expression of N-acetylgalactosamine 4-sulfate 6-O-sulfotransferase involved in chondroitin sulfate synthesis is responsible for pulmonary metastasis. BioMed Res. Int. *2013*, 656319.
12. Li, F., Ten Dam, G.B., Murugan, S., Yamada, S., Hashiguchi, T., Mizumoto, S., Oguri, K., Okayama, M., van Kuppevelt, T.H., and Sugahara, K. (2008). Involvement of highly sulfated chondroitin sulfate in the metastasis of the Lewis lung carcinoma cells. J. Biol. Chem. *283*, 34294–34304.
13. Watanabe, K., Arumugam, S., Sreedhar, R., Thandavarayan, R.A., Nakamura, T., Nakamura, M., Harima, M., Yoneyama, H., and Suzuki, K. (2015). Small interfering RNA therapy against carbohydrate sulfotransferase 15 inhibits cardiac remodeling in rats with dilated cardiomyopathy. Cell. Signal. *27*, 1517–1524.
14. Suzuki, K., Arumugam, S., Yokoyama, J., Kawauchi, Y., Honda, Y., Sato, H., Aoyagi, Y., Terai, S., Okazaki, K., Suzuki, Y., et al. (2016). Pivotal role of carbohydrate sulfotransferase 15 in fibrosis and mucosal healing in mouse colitis. PLoS ONE *11*, e0158967.

15. Suzuki, K., Yokoyama, J., Kawauchi, Y., Honda, Y., Sato, H., Aoyagi, Y., Terai, S., Okazaki, K., Suzuki, Y., Sameshima, Y., et al. (2016). Phase 1 clinical study of siRNA targeting carbohydrate sulfotransferase 15 in Crohn's disease patients with active mucosal lesions. J. Crohns Colitis, Published online August 1, 2016. http://dx.doi.org/10.1093/ecco-jcc/jjw143.

16. Fire, A., Xu, S., Montgomery, M.K., Kostas, S.A., Driver, S.E., and Mello, C.C. (1998). Potent and specific genetic interference by double-stranded RNA in Caenorhabditis elegans. Nature *391*, 806–811.

17. Senoo, T., Hattori, N., Tanimoto, T., Furonaka, M., Ishikawa, N., Fujitaka, K., Haruta, Y., Murai, H., Yokoyama, A., and Kohno, N. (2010). Suppression of plasminogen activator inhibitor-1 by RNA interference attenuates pulmonary fibrosis. Thorax *65*, 334–340.

18. D'Alessandro-Gabazza, C.N., Kobayashi, T., Boveda-Ruiz, D., Takagi, T., Toda, M., Gil-Bernabe, P., Miyake, Y., Yasukawa, A., Matsuda, Y., Suzuki, N., et al. (2012). Development and preclinical efficacy of novel transforming growth factor-β1 short interfering RNAs for pulmonary fibrosis. Am. J. Respir. Cell Mol. Biol. *46*, 397–406.

19. Leask, A., and Abraham, D.J. (2003). The role of connective tissue growth factor, a multifunctional matricellular protein, in fibroblast biology. Biochem. Cell Biol. *81*, 355–363.

20. Allen, J.T., Knight, R.A., Bloor, C.A., and Spiteri, M.A. (1999). Enhanced insulin-like growth factor binding protein-related protein 2 (connective tissue growth factor) expression in patients with idiopathic pulmonary fibrosis and pulmonary sarcoidosis. Am. J. Respir. Cell Mol. Biol. *21*, 693–700.

21. Chien, J.W., Richards, T.J., Gibson, K.F., Zhang, Y., Lindell, K.O., Shao, L., Lyman, S.K., Adamkewicz, J.I., Smith, V., Kaminski, N., and O'Riordan, T. (2014). Serum lysyl oxidase-like 2 levels and idiopathic pulmonary fibrosis disease progression. Eur. Respir. J. *43*, 1430–1438.

22. Barry-Hamilton, V., Spangler, R., Marshall, D., McCauley, S., Rodriguez, H.M., Oyasu, M., Mikels, A., Vaysberg, M., Ghermazien, H., Wai, C., et al. (2010). Allosteric inhibition of lysyl oxidase-like-2 impedes the development of a pathologic microenvironment. Nat. Med. *16*, 1009–1017.

23. Lukacs, N.W., Chensue, S.W., Smith, R.E., Strieter, R.M., Warmington, K., Wilke, C., and Kunkel, S.L. (1994). Production of monocyte chemoattractant protein-1 and macrophage inflammatory protein-1 alpha by inflammatory granuloma fibroblasts. Am. J. Pathol. *144*, 711–718.

24. Smith, R.E., Strieter, R.M., Zhang, K., Phan, S.H., Standiford, T.J., Lukacs, N.W., and Kunkel, S.L. (1995). A role for C-C chemokines in fibrotic lung disease. J. Leukoc. Biol. *57*, 782–787.

25. David, G., Lories, V., Heremans, A., Van der Schueren, B., Cassiman, J.J., and Van den Berghe, H. (1989). Membrane-associated chondroitin sulfate proteoglycans of human lung fibroblasts. J. Cell Biol. *108*, 1165–1173.

26. Mizumoto, S., Yamada, S., and Sugahara, K. (2015). Molecular interactions between chondroitin-dermatan sulfate and growth factors/receptors/matrix proteins. Curr. Opin. Struct. Biol. *34*, 35–42.

27. Xu, X., Chen, H., Zhu, X., Ma, Y., Liu, Q., Xue, Y., Chu, H., Wu, W., Wang, J., and Zou, H. (2013). S100A9 promotes human lung fibroblast cells activation through receptor for advanced glycation end-product-mediated extracellular-regulated kinase 1/2, mitogen-activated protein-kinase and nuclear factor-κB-dependent pathways. Clin. Exp. Immunol. *173*, 523–535.

28. van Dijk, E.M., Menzen, M.H., Spanjer, A.I., Middag, L.D., Brandsma, C.A., and Gosens, R. (2016). Noncanonical WNT-5B signaling induces inflammatory responses in human lung fibroblasts. Am. J. Physiol. Lung Cell. Mol. Physiol. *310*, L1166–L1176.

29. Robbins, M., Judge, A., and MacLachlan, I. (2009). siRNA and innate immunity. Oligonucleotides *19*, 89–102.

30. Xia, Y., Entman, M.L., and Wang, Y. (2013). CCR2 regulates the uptake of bone marrow-derived fibroblasts in renal fibrosis. PLoS ONE *8*, e77493.

31. Baran, C.P., Opalek, J.M., McMaken, S., Newland, C.A., O'Brien, J.M., Jr., Hunter, M.G., Bringardner, B.D., Monick, M.M., Brigstock, D.R., Stromberg, P.C., et al. (2007). Important roles for macrophage colony-stimulating factor, CC chemokine ligand 2, and mononuclear phagocytes in the pathogenesis of pulmonary fibrosis. Am. J. Respir. Crit. Care Med. *176*, 78–89.

32. O'Riordan, T.G., Smith, V., and Raghu, G. (2015). Development of novel agents for idiopathic pulmonary fibrosis: progress in target selection and clinical trial design. Chest *148*, 1083–1092.

33. Takakura, K., Shibazaki, Y., Yoneyama, H., Fujii, M., Hashiguchi, T., Ito, Z., Kajihara, M., Misawa, T., Homma, S., Ohkusa, T., and Koido, S. (2015). Inhibition of cell proliferation and growth of pancreatic cancer by silencing of carbohydrate sulfotransferase 15 in vitro and in a xenograft model. PLoS ONE *10*, e0142981.

34. Ashcroft, T., Simpson, J.M., and Timbrell, V. (1988). Simple method of estimating severity of pulmonary fibrosis on a numerical scale. J. Clin. Pathol. *41*, 467–470.

35. Itakura, M., Tokuda, A., Kimura, H., Nagai, S., Yoneyama, H., Onai, N., Ishikawa, S., Kuriyama, T., and Matsushima, K. (2001). Blockade of secondary lymphoid tissue chemokine exacerbates Propionibacterium acnes-induced acute lung inflammation. J. Immunol. *166*, 2071–2079.

36. Kakugawa, T., Mukae, H., Hayashi, T., Ishii, H., Abe, K., Fujii, T., Oku, H., Miyazaki, M., Kadota, J., and Kohno, S. (2004). Pirfenidone attenuates expression of HSP47 in murine bleomycin-induced pulmonary fibrosis. Eur. Respir. J. *24*, 57–65.

37. Fujii, M., Shibazaki, Y., Wakamatsu, K., Honda, Y., Kawauchi, Y., Suzuki, K., Arumugam, S., Watanabe, K., Ichida, T., Asakura, H., and Yoneyama, H. (2013). A murine model for non-alcoholic steatohepatitis showing evidence of association between diabetes and hepatocellular carcinoma. Med. Mol. Morphol. *46*, 141–152.

38. Hattori, N., Mizuno, S., Yoshida, Y., Chin, K., Mishima, M., Sisson, T.H., Simon, R.H., Nakamura, T., and Miyake, M. (2004). The plasminogen activation system reduces fibrosis in the lung by a hepatocyte growth factor-dependent mechanism. Am. J. Pathol. *164*, 1091–1098.